View metadata, citation and similar papers at core.ac.uk

brought to you by CORE

provided by UNT Digital Library

LAWRENCE
LIVERMORE
NATIONAL
LABORATORY

UCRL-JRNL-217812

Characterization and Source Term Assessments of Radioactive Particles from Marshall Islands Using Non-Destructive Analytical Techniques

J. Jernstrom, M. Eriksson, R. Simon, G. Tamborini, O. Bildstein, R. Carlos-Marquez, S. R. Kehl, M. Betti, T. Hamilton

December 20, 2005

Spectrochemica Acta Part B

Disclaimer

This document was prepared as an account of work sponsored by an agency of the United States Government. Neither the United States Government nor the University of California nor any of their employees, makes any warranty, express or implied, or assumes any legal liability or responsibility for the accuracy, completeness, or usefulness of any information, apparatus, product, or process disclosed, or represents that its use would not infringe privately owned rights. Reference herein to any specific commercial product, process, or service by trade name, trademark, manufacturer, or otherwise, does not necessarily constitute or imply its endorsement, recommendation, or favoring by the United States Government or the University of California. The views and opinions of authors expressed herein do not necessarily state or reflect those of the United States Government or the University of California, and shall not be used for advertising or product endorsement purposes.

Characterization and Source Term Assessments of Radioactive Particles from Marshall Islands Using Non-Destructive Analytical Techniques

J. Jernström, M. Eriksson[*], R. Simon[#], G. Tamborini[@], O. Bildstein[@], Carlos Marquez[@], S.R. Kehl[$], M. Betti[@], and T.F. Hamilton[$]

Laboratory of Radiochemistry, University of Helsinki, P.O. Box 55, FIN-00014, University of Helsinki, Finland; *IAEA-MEL, International Atomic Energy Agency-Marine Environment Laboratory, 4 Quai Antoine 1er, MC 98000 Monaco, Principality of Monaco; [#]Institute for Synchrotron Radiation, Forschungszentrum Karlsruhe GmbH, D-76021 Karlsruhe, Germany; [@]European Commission, Joint Research Centre, Institute for Transuranium Elements, P.O. Box 2340, D-76125 Karlsruhe, Germany; [$]Lawrence Livermore National Laboratory, PO Box 808, Livermore, CA 94551-0808, U.S.A.

Abstract–A considerable fraction of radioactivity entering the environment from different nuclear events is associated with particles. The impact of these events can only be fully assessed where there is some knowledge about the mobility of particle bound radionuclides entering the environment. The behavior of particulate radionuclides is dependent on several factors, including the physical, chemical and redox state of the environment, the characteristics of the particles (e.g., the chemical composition, crystallinity and particle size) and on the oxidative state of radionuclides contained in the particles. Six plutonium-containing particles stemming from Runit Island soil (Marshall Islands) were characterized using non-destructive analytical and microanalytical methods. By determining the activity of ^{239,240}Pu and ^{241}Am isotopes from their gamma peaks structural information related to Pu matrix was obtained, and the source term was revealed. Composition and elemental distribution in the particles were studied with synchrotron radiation based micro X-ray fluorescence (SR-μ-XRF) spectrometry. Scanning electron microscope equipped with energy dispersive X-ray detector (SEM-EDX) and secondary ion mass spectrometer (SIMS) were used to examine particle surfaces. Based on the elemental composition the particles were divided into two groups; particles with plain Pu matrix, and particles where the plutonium is included in Si/O-rich matrix being more heterogenously distributed. All of the particles were identified as fragments of initial weapons material. As containing plutonium with low ^{240}Pu/^{239}Pu atomic ratio, ~2-6 %, which corresponds to weapons grade plutonium, the source term was identified to be among the safety tests conducted in the history of Runit Island.

1. Introduction

From 1946 through 1958 the United States conducted a total of 65 atmospheric nuclear weapons tests on Bikini and Enewetak Atolls within the Republic of the Marshall Islands [UNSCEAR 2000; Hamilton, 2004]. The nuclear test program included air drops (4), barge detonations (35), tower detonations (13), surface detonations (10), and underwater detonations (3). The total yield for all tests conducted on Bikini and Enewetak Atolls was 109 Mt with an estimated fission yield of 53 % [UNSCEAR, 2000; Hamilton 2004]. At Bikini, the total yield was approximately 76.8 Mt with a fission yield of approximately 55 %. At Enewetak, the total and fission yields were 30.2 Mt and 49%, respectively [UNSCEAR, 2000]. A surface safety test and one additional unsuccessful detonation at Enewetak Atoll resulted in little of no fission yield [DOE, 2000].

The nuclear test program in the Marshall Islands produced both global and localized forms of fallout contamination. The terrestrial and marine environments of each atoll are contaminated with a range of fission and activation products, and unfissioned nuclear materials [Hamilton, 2004]. Today, quantities of fission products such as cesium-137 (^{137}Cs), strontium-90 (^{90}Sr) and europium-155 (^{155}Eu); activation products such as iron-55 (^{55}Fe), cobalt-60 (^{60}Co) and bismuth-207 (^{207}Bi), and transuranic elements such as plutonium-238,239,240,241 (^{238,239,240,241}Pu) and americium-241 (^{241}Am) are known to persist in the environment. The largest inventory of residual plutonium is associated with atoll lagoon sediments [Noshkin et al., 1987].

It has been estimated that at Bikini the sediments contain about 17 TBq of ^{239,240}Pu and 14 TBq of ^{241}Am to a depth of 2 cm, and approximately 120 TBq of ^{239,240}Pu and 100 TBq of ^{241}Am in associated with sediment layers to greater depths [Noshkin et al., 1997]. At Enewetak Atoll (including the region around Runit Island) the estimated sediment inventories for ^{239,240}Pu and ^{241}Am, are 9.2 TBq and 2.8 TBq, repectively, in the surface layer, and 44.2 TBq and 17.6 TBq, respectively, to a depth of 16 cm [Noshkin and Robison, 1997].

The measured ^{240}Pu/^{239}Pu isotopic ratio in soil samples from Bikini Atoll is around ~0.3 [Muramatsu et al., 2001]. This value is substantially higher compared to the ratio in integrated global fallout, 0.176 ± 0.014 [Krey et al., 1976]. Isotopic ratios from 0.318 to 0.338 have also been measured in fallout debris from the Castle *Bravo* thermonuclear test (15 Mt, yield 66%) [Komura et al., 1984]. The Bravo test, conducted on Bikini Atoll in March of 1954, was the single most important contaminating event in the Marshall Islands and was responsible for widespread fallout contamination of Bikini Atoll as well as other atolls to the east of Bikini. In the study conducted by Muramatsu et al. (2001), the lowest ^{240}Pu/^{239}Pu isotopic ratio measured in surface soils from the Marshall Islands was around ~0.065 and is consistent with that observed in weapons grade plutonium. This particular soil sample was collected from Runit Island on Enewetak Atoll in a region impacted by close-in fallout from the *Quince* and *Fig* tests. The *Quince* safety test was conducted in August of 1958 where the high explosive component of the device was detonated but there was no fission yield. As a consequence, large quantities of plutonium fuel particles were dispersed into the local environment. [Hamilton et al., 2005; Noshkin and Robison, 1997].

In general, a considerable fraction of radioactivity entering the environment from nuclear events such as nuclear weapons accidents, authorized or accidental releases of radioactive effluent and in nuclear weapon detonations is associated with particles. The size distribution of these radioactive particles or aggregates is typically log-normal [Eriksson, 2002; Shevchenko, 2004], i.e., most of the activity is carried by relatively few larger-sized particles. As such, the impact of nuclear events can only be fully assessed where there is some knowledge about the mobility of particle bound radionuclides entering the environment. The behavior of particulate radionuclides is dependent on several factors, including the physical, chemical and redox state of the environment, the characteristics of the particles (e.g., the chemical composition, crystallinity and particle size) and on the oxidative state of radionuclides contained in the particles [Salbu et al., 2004]. In order to extend our knowledge of the mobilization and weathering of radionuclides in the environment, we have developed a series of non-destructive analytical techniques to help for characterizing the nature, chemical composition and size of radioactive particles [Jernström et al., 2004; Eriksson et al., 2005].

In the current study, six radioactive particles were separated from bulk soil samples collected from Runit Island on Enewetak Atoll (Hamilton et al., 2005) and characterized using scanning electron microscope equipped with energy dispersive X-ray spectrometer (SEM-EDX), synchrotron radiation based micro X-ray fluorescence (SR-μ-XRF) spectrometry, gamma spectrometry and secondary ion mass spectrometry (SIMS). A beta camera was also used to find the exact location of the particles separated on carbon base tape. Particles were visualized, and the morphology and surface elemental composition studied with SEM-EDX. The elemental composition of the particles was determined with SR-μ-XRF, and the gamma lines of ^{239}Pu, ^{240}Pu and ^{241}Am measured by gamma spectrometry. Surface isotopic composition was studied with SIMS. The results were then compared with published data for particles collected from other sites or under different release conditions.

2. Materials and Methods

Lawrence Livermore National Laboratory (LLNL) collected the original soil samples from Runit Island on Enewetak Atoll in the Marshall Islands during November of 2000. The soil samples were stored frozen and returned to Livermore for processing. Details concerning the field sampling and the initial isolation of high-activity particles analyzed in this study are given elsewhere [Hamilton et al., 2005]. Briefly, the soil samples were oven dried at 60°C and split into 50 g aliquots. The presence of high-activity particles in selected 50 g aliquots of soil could easily be identified using

the 59.54 keV energy peak from ^{241}Am using a portable SAM 925 gamma spectrometry unit from Berkeley Nucleonics, Inc. High-activity samples were further split and the presence of any particles tracked until the matrix was reduced to a mass of less than 50-250 mg. The frequency distribution of high-activity particles as well as the activity concentration of plutonium in the bulk soil and various dry-sieved soil fractions are described elsewhere [Hamilton et al., 2005]. The activity concentration of $^{239+240}$Pu in the bulk soil matrix after removal of the high-activity particles was approximately 1.5 kBq kg^{-1}, dry soil.

2.1 Isolation of radioactive particles

Under this study, the high-activity particle samples obtained from LLNL were further searched at Institute for Transuranium Elements (ITU) using a sample splitting technique until only a few grains (~μg) remained [Eriksson et al., 2002]. The grains were then attached to a piece of adhesive carbon tape (Plano, Germany) and the tape mounted on an aluminium frame compatible for use with our analytical instrumentation. The exact location of any high-activity particles was revealed with a beta camera.

2.2 Beta camera

The Beta Camera is a detector for on-line digital detection of charged particles (α, β particles and conversion electrons) and low energy X-rays from thin samples. The sample is mounted in close contact to a thin scintillator on top of an image photon detector. The Beta Camera has better sensitivity than normal autoradiography films, and has a spatial resolution of ~0.5 mm [Ljunggren, 2003]. This technique is very fast; a Pu-containing particle with activity of 2 Bq can be localized in less than 30 minutes. This is faster compared to film autoradiography and does not need processing before the radionuclide content or radioactive particle distribution within the sample is determined. In general, this device has been proven to be a very useful tool to localize and identify radioactive particles released to the environment [Eriksson et al., 2002].

2.3 Gamma spectrometry

The particles were decay measured with a n-doped planar HP(Ge) detector equipped with a Be-window (EG&G ORTEC, USA). The detector has an energy resolution (full width at half maximum, FWHM) of 530 eV at 122 keV. Detector calibration was done with a mixed nuclide point source (diameter 8 mm, GL574, AEA Technology QSA GmbH, Germany) which offers the lowest energy of 59.54 keV from ^{241}Am. The energy and branching ratio data used in gamma analysis was obtained from The Lund/LBNL Nuclear Data Search database [Chu et al., 1999]. The detector is cooled with liquid N_2 and provided with a voltage of -2000 V from a high voltage supply (EG&G Ortec 659). The pulses obtained from the HP(Ge) detector were magnified and shaped by a spectroscopy amplifier (Canberra 2021) and analysed in the multichannel buffer (EG&G Ortec, Ethernim 919E). The spectra were acquired with GammaVision32 (EG&G Ortec) software. The detector is placed in a properly ventilated room, and is shielded with 5 cm of lead with low content of ^{210}Pb.

2.4 Scanning electron microscope (SEM)

Radioactive particles were studied using an automatic SEM equipped with an energy dispersive X-ray (EDX) spectrometer (PERSONAL SEM®, RJ Lee Group, Inc., USA). The particles lay on conducting carbon tape mounted on an aluminium frame. No conductive coating which would give problems in the SIMS measurements was needed. To search for particles containing high atomic numbers, the samples were scanned using backscattered mode. By focusing a small spot on the high Z area, and by analyzing the X-ray fluorescence signal with EDX, the X-ray lines could be identified and the elemental composition derived. The applied voltage was 20 kV, and the working distance (filament - sample) was between 16-18 mm.

2.5 Micro X-ray fluorescence (μ-XRF) spectrometry

The radioactive particles were measured at the Fluo-Topo beamline at the Synchrotron Radiation Facility ANKA situated in Karlsruhe, Germany [Simon et al., 2003]. The white beam of a bending magnet was monochromatised by a W-BC_4 multilayer double monochromator to 23.2±0.3 keV.

The excitation energy was chosen in order to excite the L core electrons of U and Pu. An ellipsoidal glass monocapillary (IfG, Germany) was employed for focusing a beam of 1 mm × 1 mm down to a spot size of 22.9 μm in diameter. An energy dispersive OXFORD Si(Li) detector with a FWHM of 133 eV at 5.9 keV was placed in 90° geometry with respect to the incoming beam to minimise the amount of scattered photons reaching the detector.

Elemental maps were produced from scans over individual particles. Step size varied from 10 μm to 50 μm, depending on the size of the particle. Spectral acquisition time was 10 s. The obtained intensities were normalized with beam current and live time. Spectral analysis was performed with an AXIL software program [Vekemans et al., 1994]. The energies and relative intensities of the L and M line series of plutonium have been added to the X-ray library of AXIL, based on a database of X-ray transition energies [Deslattes et al., 2003].

2.6 Secondary ion mass spectrometry (SIMS)

SIMS studies were conducted with a double-focusing CAMECA IMS 6f (Courbevoie, France) spectrometer. The instrument has been engineered for fast switching between masses and it possesses two microfocus ion sources. These sources can be used either in microscope or microprobe mode [Tamborini et al., 1998]. During the analysis, the samples were sputtered with a primary O^{2+} beam of 15 keV (±0.5%) with a current intensity between 1 nA and 2 nA, and a diameter of a few μm. In the microprobe mode an area of 250 μm × 250 μm on the sample surface was rastered. Positive secondary ions were accelerated to 5 keV and intensity controlled by tuning of the primary ion beam current. The energy window was adjusted between 40 eV and 50 eV to reduce molecular ion contributions. The instrument can typically operate with a mass resolution power (MRP) of 25000. However, for measurements of uranium and plutonium isotopes, a MRP of 1000 is sufficient. With this resolution, flat-top peaks were obtained, improving the accuracy of the measurements. The ions were counted with an electron multiplier in the ion counting mode. The electron multiplier is used to measure count rates in the range of 10^{-6} - 10^{-1} cps. The instrument allows the detection of ~5×10^{9} atoms of U and ~1.5×10^{9} atoms of Pu.

Mass calibration was performed using synthetic monodispersive uranium oxide particles [Erdmann et al., 2000; Tamborini, 2004] as standards, and uranium isotopes ^{234}U, ^{235}U and ^{238}U were measured before each analysis. For Pu containing particles, the mass spectrometer was set to mass 239.0522 or 240.0538.

3. Results and discussion

The particles varied with size, morphology and surface composition. Three of them, particles ‘D’, ‘E’ and ‘F’, were covered with silicon- and oxygen-rich material. When observed with optical microscope the coating looked semi-transparent and glasslike, containing small bubblelike inclusions. Three of the particles, ‘A’, ‘B’ and ‘C’, were free of coating, exposing a surface rich with plutonium. A common factor with the particles was that the covered ones were notably larger in size than the uncovered ones. Details of size and surface of the particles are introduced in Table 1.

3.1 Gamma spectrometry

The n-doped HP(Ge) detector allowed determination of $^{239,240}Pu$ and ^{241}Am activities from their gamma lines. Two lines from ^{239}Pu at energies of 38.66 keV (Iγ: 0.0105 %, $T_{1/2}$: 24110 a) and 51.62 keV (Iγ: 0.0271 %), one gamma line from ^{240}Pu (45.24 keV, 0.0450 %, $T_{1/2}$: 6563 a) and two gamma lines from ^{241}Am (26.34 keV, 2.4 % and 59.54 keV, 35.9 %, $T_{1/2}$: 432.2 a) were analyzed to reveal activities and atomic ratios between different isotopes. The efficiency calibration of the detector was done with the certified GL574 mixed nuclide point source.

Detected gamma emission originates from the whole particle. Therefore, by taking into account attenuation of different gamma energies in the particle matrix it is possible to obtain information of matrix homogeneity by comparing the results with those obtained from SIMS measurements, which reveal surface-related information. In the activity analysis of each particle the photon attenuation was taken into account by conducting efficiency calibration using the 26.34 keV and 59.54 keV lines of ^{241}Am. The efficiency for the lower energy photons (26.34 keV) was in all cases between 22.8 % and 15.1 % less than for the 59.54 keV photons: 20.5-22.8 % less in the case of the smaller sized

particles ‘A-C’ and 15.1-18.7 % less with the larger sized particles ‘D-F’ (Table 2). This indicates that the ^{241}Am photons originating from the smaller, uncovered particles are more attenuated compared to the photons emitted from the larger particles.

In the smaller particles the observed attenuation is mostly due to self absorption of photon energy caused by high Z matrix of high density. Using the Lambert-Beer law as shown below it is possible to calculate the thickness of particle matrix when the relative attenuation of the two photons due to the matrix is known.

$$I = I_0 \times \exp[-\mu \times x]$$

where I_0 is the incident flux, μ is the linear absorption coefficient (obtained from the XCOM: Photon Cross Section Database [Berger et al., 1999]), and x is the matrix thickness. In the three particles ‘A-C’ the matrix thickness was calculated to be 21.1-23.7 µm with PuO_2, and 18.6-20.9 µm with metallic Pu.

In the larger particles ‘D-F’ the photon attenuation arises from both Pu matrix and silicon/oxygen-rich material. By considering the fact that the ^{241}Am photons are more attenuated in the smaller particles it can be suggested that Pu inside the larger particles exists either in thinner, flakelike structure, or is spreaded in the particle matrix.

Determination of plutonium activity from the low intensity peaks has large uncertainties. This can be seen in Tables 3 and 4 where different activities and atomic ratios between Pu and Am isotopes are presented. In the spectral analysis procedure a region of interest (ROI) within a gamma peak was chosen, and the net peak area was determined by the WAN32 analysis engine of the GammaVision program. To take into account significant peak intensity variations observed with different ROIs within the low intensity plutonium peaks multiple ROIs were chosen. The final activities of the Pu isotopes were then taken as the average of the activities calculated from analysis with different ROIs (Table 3). The activity uncertainties reflect to the counting statistics, and were determined using the 2 sigma standard error equation for inefficient statistics:

$$m_{\bar{x}} = \frac{m}{\sqrt{n}} = \sqrt{\frac{\sum\left(x_i - \bar{x}\right)^2}{n(n-1)}}$$

The atomic ^{240}Pu/^{239}Pu and ^{241}Am/^{239,240}Pu ratios (Table 4) were calculated from the average activity values. The adjacent Pu ratios obtained from SIMS measurements are much more consistent, however, being situated at the same level, indicating the source term to be weapons grade Pu, which has ^{240}Pu/^{239}Pu atomic ratio of < 7 %. Muramatsu et al. (2001) found ^{240}Pu/^{239}Pu isotopic ratios of 6.5 % in surface soil samples from Runit Island at Enewetak Atoll, connecting the findings to weapons grade Pu from a safety test conducted in the island´s past.

The observation that the spectra of all the three uncovered particles do not contain any peaks from fission products also supports the suggestion of a nonfissile source term. A weak ^{137}Cs (661.657 keV, 85.1 %) peak was observed in the spectrum of the covered particles, as can be seen in the gamma spectrum of the particle ‘E’ in Fig. 1. The $^{239+240}$Pu/^{137}Cs activity ratio (12/2004) was determined to be ~2500 for particle ‘E’ and ~4400 for particle ‘F’. The cesium peak in the spectrum of the particle ‘D’ was hardly discernible, and had statistically too low amount of pulses for analysis. The obtained ratios are considerably higher than the ones presented in an earlier study. Muramatsu et al. (2001) report the $^{239+240}$Pu/^{137}Cs activity ratio to be 34.7 in Runit Island soil, and 0.09-0.17 in Bikini Atoll soil. However, these ratios were determined from bulk samples instead of from single particles, therefore the activity ratios reflect to more than one source term. By considering the findings it is possible to deduce that either the ^{137}Cs activity exists in the particle cover material, or the larger particles originate from a source where nuclear fission has taken place, *i.e.*, nuclear explosion with minor fission yield.

3.2 Scanning electron microscope (SEM)

Three particles (‘A-C’, left side images in Fig. 2a) were irregularely shaped, expressing Pu-rich surface with in places minor amounts of silicon. Any americium signal was not detected, due to low elemental concentration in the particles. Calcium, with minor amounts of oxygen and magnesium, were observed to partly cover the particles (Table

1). The composition of soil in Runit Island, as well as in Marshall Islands in general, is mainly calcium carbonate ($CaCO_3$) with some aragonite ($MgCO_3$) [Robison et al., 1999], which explains the observation. Due to use of 20 keV electron beam Pu-L lines were not efficiently enough excited to be detectable. Instead, the M lines of Pu are clearly visible in the X-ray fluorescence spectra in Figs. 2a and 2b, with overlap between Pu-Mγ and Ca-Kα lines at ~3.7 keV. U-M lines partly overlap with M lines of Pu; however, no uranium was detected from any of the six particles. This differs from the U/Pu -containing particles [Eriksson et al., 2005] originating from the Thule aircraft accident (in 1968), where nuclear weapons were nonfissionably exploded.

Detailed visual investigation of the larger, coated particles ('D-F', left side images in Fig. 2b) was difficult as the particles protruded from the conducting base high enough to result charging effects. The glasslike coating contained mainly Si and O, and less amounts of Al, Ca, Mg and Na (Table 1). Any plutonium signal could not be detected due to the covering substance or because the Pu concentration in the matrix was too low to be detected by the EDX system used.

This finding has important implications for assessing the long-term health and ecological impacts of residual fallout contamination from the *Quince* and *Fig* tests. For example, the coated particles may be less susceptible to weathering and, therefore, the particle bound radionuclides may be much less available for biological uptake through the local food chain [Hamilton et al., 2005].

The surface composition of the larger particles 'D-F' with Si and O as major elemental constituents differs from the consistency of the calcareous Runit Island soil, suggesting the coating of the particles to originate from the structure of the exploded weapon. No elements being commonly present in Pu weapon structure, *i.e.*, iron, lead, bismuth and uranium, were observed in the X-ray spectra of the particles. This indicates that instead of being formed due to the high-temperature explosion the particles are fragments of the initial weapon material.

3.3 Micro X-ray fluorescence (μ-XRF) spectrometry

Intensity maps showing the plutonium distribution in the six particles are presented in Figs. 2a and 2b, in the right-side columns adjacent to the corresponding SEM images. No americium signal was detected due to low elemental concentration in the particles. As can be seen from the images in Fig. 2a the particles 'A-C' have a homogenous plutonium distribution. This differs from the larger particles 'D-F', where the Pu concentration look more heterogenously distributed (Fig. 2b). This can be an effect of different attenuation of the characteristic Pu X-rays as the fluorescenced photons in the particles have differing distances to pass to the detector in the irregularly shaped large particles. Part of the fluorescence data is missing in the particle 'E' due to loss of synchrotron beam during the scan.

Based on the observations from the analysis with gamma and μ-XRF spectrometry it is not possible to clarify the exact form of plutonium in the larger particles 'D-F'. It can exist as particle-like structure, or it can be distributed in the Si/O -rich matrix. Methods which reveal three-dimensional structural information, such as XRF tomography, would be useful in studying this question [Wegrzynek et al., 2005].

3.4 Secondary ion mass spectrometry (SIMS)

SIMS measurements were able to be conducted on three of the six particles; on the small sized particles 'A-C'. No measurements could be performed on the particles 'D-F', because of charging effects and the unsuitability of the particle surface for the analysis. The non-conducting glasslike particle matrix was charged on the surface by the primary O^{2+} ion beam. This effect destroys the electrostatic field that extracts the secondary ions from the sample surface into the mass spectrometer. In addition, the roughness and non-flatness of the sample surface makes it difficult to focus the primary ion beam on a spot of a particle. Focusing of the beam is usually performed on the sample surface, *i.e.*, on the level of the carbon tape. For the three covered samples 'D-F' the focusing surface is situated significantly below the spot of the samples to be analysed. This produces an unfocused beam which cannot be used for analyses.

The $^{240}Pu/^{239}Pu$ atomic ratios of the particles 'A-C' are all around 6 % (Table 4), indicating the

presence of weapons grade plutonium. However, it might be expected that this ratio is slightly overestimated. A recent SIMS study conducted with U/Pu particles stemming from the Thule accident showed that the raster size used during the analysis has an effect on the $^{240}Pu/^{239}Pu$ ratio [Ranebo et al., 2005]. In this study it is suggested that the sample support (carbon tape on Al frame) introduces a mass isobaric interference at mass 240, therefore producing a biased 240/239 mass ratio. To avoid this Ranebo et al. (2005) suggest that raster size should be smaller than the size of the particle.

In the present study with the Runit Island particles raster size of 250 µm × 250 µm was used. This size well exceeds the area of all the three analyzed particles; approximately 24 times in case of the particle 'A'; 23 and 43 times with the particles 'B' and 'C', respectively. Ranebo et al. (2005) found ~10-15 % increase in the 240/239 ratio when the raster size exceeded 50 times the raster size fitting within the particle. This might indicate that the ratios shown in Table 4 are slightly too high, however, not at the level of the ratios obtained from the measurements with gamma spectrometry.

To reveal possible isobaric interferences a mass spectrum was measured on all of the three particles. One of the spectra is presented in Fig. 3. Additionally for the Pu masses 239 and 240 were measured the mass 241 together with U isotopic masses of 234, 235, 236, 238. The mass peak at 241 contain both 241Am and 241Pu. However, as the relative sensitivity factor for these elements was not known they have been excluded from the result treatment. As can be seen in Fig. 3 the amount of the U isotopes is close to zero.

4. Conclusions

Plutonium-containing particles collected from Runit Island soil on Enewetak Atoll in the northern Marshall Islands were characterized and studied using various analytical and microanalytical methods. The used techniques, which included gamma spectrometry, scanning electron microscopy, synchrotron radiation based X-ray fluorescence spectrometry and secondary ion mass spectrometry, revealed information and details related to structural and elemental properties of the particles. All these techniques are non-destructive; after the analysis the particles are still intact for further studies.

Two types of Pu particles were found in respect to elemental composition. One group contained particles with mainly plain Pu matrix, whereas in the particles of the other group plutonium was included in matrix rich with silicon and oxygen. It is concluded that also the Si/O-rich particles are fragments of the initial weapon material. This is supported by the facts that no traces of other elements which are common in the weapon structure were found, and the particle matrix differs significantly from the calcareous soil environment.

Common for all the particles was the low $^{240}Pu/^{239}Pu$ atomic ratio (between 0.02 and 0.06) indicating no fission of the material. However, in the Si/O-rich particles trace of ^{137}Cs could be detected. The most likely source term for these types of particles is the *Fig* safety test or other low-yield test events conducted in the vicinity of Runit Island.

ACKNOWLEDGEMENT

This work was performed under auspices of the U.S. Department of Energy by University of California, Lawrence Livermore National Laboratory under Contract W-7405-Eng-48. Mr. Marshall Stuart (LLNL) assisted with the sample collection and the initial isolation of radioactive particles. The IAEA is grateful for the support provided to its Marine Environment Laboratory by the Government of the Principality of Monaco. The authors would also like to thank Dr. Kaj Ljunggren for the use of the Beta Camera at Lund University, Sweden.

REFERENCES

Berger, M.J., Hubbell, J.H., Seltzer, S.M., Coursey, J.S., and Zucker, D.S. (1999), XCOM: Photon cross section database (version 1.2). [Online] Available: http://physics.nist.gov/xcom [2005, March 30]. National Institute of Standards and Technology, Gaithersburg, MD.

Chu, S. Y. F., Ekström, L. P. and Firestone, R. P. (1999), The Lund/LBNL Nuclear Data Search database, Version 2.0. URL: http://nucleardata.nuclear.lu.se/NuclearData/toi/index.asp.

Desideri, D., Meli, M. A., Roselli, C., Testa, C. and Degetto, S. (2001), Speciation of natural and antropogenic radionuclides in different sea sediment samples. Journal of Radioanalytical and Nuclear Chemistry 248 (3), 727-733.

Deslattes, R. D., Kessler, E. G., Indelicato, P., de Billy, L., Lindroth, E. and Anton, J. (2003), X-ray transition energies: new approach to a comprehensive evaluation. Reviews of Modern Physics, 75, 35-99.

Erdmann, N., Betti, M., Stetzer, O., Tamborini, G., Kratz, J. V., Trautmann, N. and van Geel, J. (2000), Production of monodisperse uranium oxide particles and their characterization by scanning electron microscopy and secondary ion mass spectrometry. Spectrochimica Acta Part B 55, 1565-1575.

Eriksson, M. (2002), On weapons plutonium in the arctic environment (Thule, Greenland). Ph.D. thesis, Risø-R-1321, Risø National Laboratory, Roskilde, Denmark, 146 p.

Eriksson, M., Ljunggren, K. and Hindorf, C. (2002), Plutonium hot particle separation techniques using real-time digital image systems, Nuclear Instruments and Methods in Physics Research Section A, 488 (1-2), 375-380.

Eriksson, M., Osán, J., Jernström, J., Wegrzynek, D., Simon, R., Chinea-Cano, E., Markowicz, A., Bamford, S., Tamborini, G., Török, S., Falkenberg, G., Alsecz, A., Dahlgaard, H., Wobrauschek, P., Streli, C., Zoeger, N. and Betti, M. (2005), Source term identification of environmental radioactive Pu/U particles by their characterisation with non-destructive analytical techniques. Spectrochimica Acta Part B, 60, 455-469.

Hamilton, T.F. (2004), Linking legacies of the Cold War to arrival of anthropogenic radionucldies in the ocean through the 20th century, In: Marine Radioactivity, (Ed. H.D. Livingston), Elsevier Ltd., 2004, pp 23-78.

Hamilton, T. F., Martinelli, R. E., Williams, R. W., Kehl, S. R., Jernström, J., Eriksson, M., Simon, R., Tamborini, G., Bildstein, O., Carlos Marquez, R. and Betti, M. (2005), A preliminary assessment of the nature and size distribution frequency of high-activity particles in soils from Runit Island, Enewetak Atoll, Science Total Environment (in preparation).

Jernstöm J., Eriksson, M., Osán, J., Tamborini, G., Török, S., Simon, R., Falkenberg, G., Alsecz, A. and Betti, M. (2004), Non-destructive characterization of low radioactive particles from Irish Sea sediment by micro X-ray synchrotron radiation techniques: micro X-ray fluorescence (μ-XRF) and micro X-ray absorption near edge structure (μ-XANES) spectroscopy. Journal of Analytical Atomic Spectrometry 19, 1428-1433.

Komura, K., Sakanoue, M. and Yamamoto, M. (1984), Determination of $^{240}Pu/^{239}Pu$ ratio in environmental samples based on the measurement of Lx/α-ray activity ratio, Health Physics, 46, 1213-1219.

Krey, P. W., Hardy, E. P., Pachuki, C., Rourke, F., Coluzza, J. and Benson, W. K. (1976), Mass isotopic composition of global fall-out plutonium in soil. Proceedings of a Symposium on Tranuranium Nuclides in the Environment 39. IAEA-SM-199-39, 671-678.

Ljunggren, K. (2003), Beta camera, Development and biomedical application. Ph.D. thesis, Lund University, Sweden.

Muramatsu, Y., Hamilton, T., Uchida, S., Tagami, K., Yoshida, S. and Robison, W. (2001), Measurement of $^{240}Pu/^{239}Pu$ isotopic ratios in soils from the Marshall Islands using ICP-MS, Science of the Total Environment, 278, 151-159.

Noshkin, V. E., Wong, K. M., Jokela, T. A., Brunk, J. L. and Eagle, R. J. (1987), Plutonium and Americium Behaviour in Coral Atoll Environments. In: Oceanic Processes in Marine Pollution, Vol. 2, (Eds. T. P. Conner, W. V. Burt and I. A. Duedall), 1987, pp. 159-174.

Noshkin, V. E. and Robison, W. L. (1997), Assessment of a radioactive waste disposal site at Enewetak Atoll, Health Physics, 73(1), 234-247.

Noshkin, V. E., Eagle, R. J., Wong, K. M. and Robison, W. L. (1997), Sediment studies at Bikini Atoll Part 2. Inventories of transuranium elements

in surface sediments, Lawrence Livermore National Laboratory, Livermore, CA, UCRL-LR-129379.

Ranebo, Y., Eriksson, M., Nedialka, N., Tamborini, G., Betti, M. and Holm, E. (2005), SIMS and SEM characterization of Pu and U environmental particles from Thule sediment. Presented at the "Advanced techniques and Radionuclide Speciation within Radioecology", IAEA-MEL, Monaco 30th September - 1st October, 2005.

Robison, W. L., Conrado, C. L., Hamilton, T. F. and Stoker, A. C. (1999), The effect of carbonate soil on transport and dose estimates for long-lived radionuclides at a U.S. Pacific test site, Lawrence Livermore National Laboratory, Livermore, CA, UCRL-JC-130231.

Salbu, B., Lind, O. C. and Skipperud, L. (2004), Radionuclide speciation and its relevance in environmental impact assessments, Journal of Environmental Radioactivity, 74, 233-242.

Shevchenko, S. V. (2004), On the uncertainty in activity measurements for samples containing “hot particles”, Applied Radiation and Isotopes 61, 1303-1306.

Simon, R., Buth, G. and Hagelstein, M. (2003), The X-ray-fluorescence facility at ANKA, Karlsruhe: Minimum detection limits and micro probe capabilities, Nuclear Instruments and Methods in Physics Research Section B, 199, 554-558.

Tamborini, G., Betti, M., Forcina, V., Hiernaut, T., Giovannone, B. and Koch, L. (1998), Application of secondary ion mass spectrometry to the identification of single particles of uranium and their isotopic measurement, Spectrochimica Acta, Part B, 53 (9), 1289-1302.

Tamborini, G. (2004), SIMS analysis of uranium and actinides in microparticles of different origin. Microchimica Acta 145, 237-242.

Vekemans, B., Janssens, K., Vincze, L., Adams, F. and van Espen, P. (1994), Analysis of X-ray spectra by iterative least squares (AXIL): new developments, X-Ray Spectrometry, 23, 278-285.

Wegrzynek, D., Markowicz, A., Bamford, S., Chinea-Cano, E. and Bogovac, M. (2005), Micro-beam X-ray fluorescence and absorption imaging techniques at the IAEA Laboratories. Nuclear Instruments and Methods in Physics Research B 231, 176-182.

United States Department of Energy (USDOE) (2000), United States Nuclear Tests: July 1945 through Sepetmber 1992, United States Department of Energy, Nevada Operations Office, Las Vegas, NV, DOE/NV-209-Rev 15.

United Nations Scientific Committee on the Effects of Atomic Radiation (UNSCEAR) (2000), *Sources and effects of ionising radiation*, United Nations Scientific Committee on the Effects of Atomic Radiation UNSCEAR 2000 Report to the General Asssembly, with Scientific Annexes, Volume 1, United Nations Publication E.94.IX.2, United Nations, New York, 2000

List of Figures

Figure 1. A gamma spectrum of the Runit Island (Marshall Islands) particle 'E', measured with a n-doped HP(Ge) detector for 66193 s. Attached in the figure is the low-energy part of the spectrum, presenting the low-energy part between the channels 100 and 1200 (5.9 - 64.6 keV). The relevant peaks used in the analysis are marked: ^{241}Am (ch. 488 / 26.34 keV), ^{239}Pu (ch. 706 / 38.66 keV), ^{240}Pu (ch. 822 / 45.24 keV), ^{239}Pu (ch. 932 / 51.62 keV) and ^{241}Am (ch. 1072 / 59.54 keV). The peak of the fission product ^{137}Cs (ch. 11936 / 661.66 keV) is discernible.

Figure 2a. The left-side column shows SEM images of particles 'A-C' with corresponding EDX spectra. The small black spot on the particle images (right side images) denotes the position where the EDX spectrum was measured. The right-side column shows μ-XRF Pu intensity maps of the same particles. The intensity maps correspond to Pu-Lα X-ray lines.

Figure 2b. The left-side column shows SEM images of the particles 'D-F' with corresponding EDX spectra. The small black spot on the particle images (right-side images) denotes the position where the EDX spectrum was measured. The right-side column shows plutonium μ-XRF intensity maps of the equivalent particles. The intensity maps correspond to Pu-Lα X-ray lines.

Figure 3. A mass spectrum of the particle 'A' measured with SIMS. The peaks at masses 239 and 240 originate from plutonium isotopes ^{239}Pu and ^{240}Pu, respectively. The peak at mass 241 is the combined content of the radionuclides ^{241}Pu and ^{241}Am. Note the very low content of the uranium isotopes 235-238.

List of Tables

Table 1. Details of size, surface type and surface composition of six radioactive particles 'A-F' separated from Runit Island (Marshall Islands) soil.

Table 2. Efficiency difference between two photon energies of ^{241}Am related to physical size and ^{241}Am activity in the studied particles.

Table 3. ^{239}Pu, ^{240}Pu and ^{241}Am activities of six Runit Island (Marshall Islands) particles measured with gamma spectrometry. The ^{239}Pu activity represents the average value obtained from the two peaks at 38.66 keV and 51.62 keV, ^{240}Pu and ^{241}Am activities are calculated from the 45.24 keV and 59.54 keV peaks, respectively.

Table 4. ^{240}Pu/^{239}Pu and ^{241}Am/^{239,240}Pu atomic ratios of the six particles 'A-F' determined with gamma spectrometry and SIMS. The particles 'D-F' were not measurable with SIMS.

Table 1.

Particle	Code	Approximate particle area (μm^2)	Surface	Surface composition
A	M21HF	2640	uncovered	Pu, O, Si, Ca (Ca, O, Mg)
B	M26JE	2690	uncovered	Pu, O, Si, Al, Ca (Ca, O, Si)
C	M37AD	1450	uncovered	Pu, O, Si, Ca (Ca, O, Mg)
D	M38CD	$1.89\ 10^5$	covered	Si, O, Al, Ca, Mg
E	M48BDB	$1.02\ 10^6$	covered	Si, O, Al, Ca, Mg
F	M54HC	$4.95\ 10^5$	covered	Si, O, Al, Ca, Na, Mg

Table 2.

Particle	Approximate particle area (μm^2)	^{241}Am (Bq)	Efficiency difference 26.34 keV / 59.54 keV (%)
A	2640	47.0 ± 0.5	20.5 ± 0.3
B	2690	45.8 ± 0.5	21.7 ± 0.3
C	1450	26.2 ± 0.3	22.8 ± 0.3
D	$1.89\ 10^5$	28.1 ± 0.3	15.1 ± 0.2
E	$1.02\ 10^6$	321.2 ± 3.6	18.7 ± 0.3
F	$4.95\ 10^5$	55.4 ± 0.6	17.5 ± 0.3

Table 3.

Particle	^{239}Pu (Bq)	^{240}Pu (Bq)	^{241}Am (Bq)
A	227 ± 30	23.3 ± 3.1	47.0 ± 0.5
B	229 ± 29	17.7 ± 2.2	45.8 ± 0.5
C	118 ± 23	15.3 ± 1.0	26.2 ± 0.3
D	129 ± 29	14.9 ± 3.0	28.1 ± 0.3
E	1615 ± 72	228 ± 25	321 ± 4
F	283 ± 38	39.8 ± 3.5	55.4 ± 0.6

Table 4.

Particle	^{240}Pu / ^{239}Pu γ-spectrometry (%)	^{240}Pu / ^{239}Pu SIMS (%)	^{241}Am / $^{239,240}Pu$ (12/2004) γ-spectrometry (%)
A	2.80 ± 0.52	6.04 ± 0.06	0.36 ± 0.10
B	2.11 ± 0.37	5.67 ± 0.07	0.35 ± 0.09
C	3.52 ± 0.72	6.31 ± 0.09	0.38 ± 0.10
D	3.15 ± 0.95	-	0.38 ± 0.16
E	3.84 ± 0.46	-	0.34 ± 0.05
F	3.84 ± 0.62	-	0.34 ± 0.08

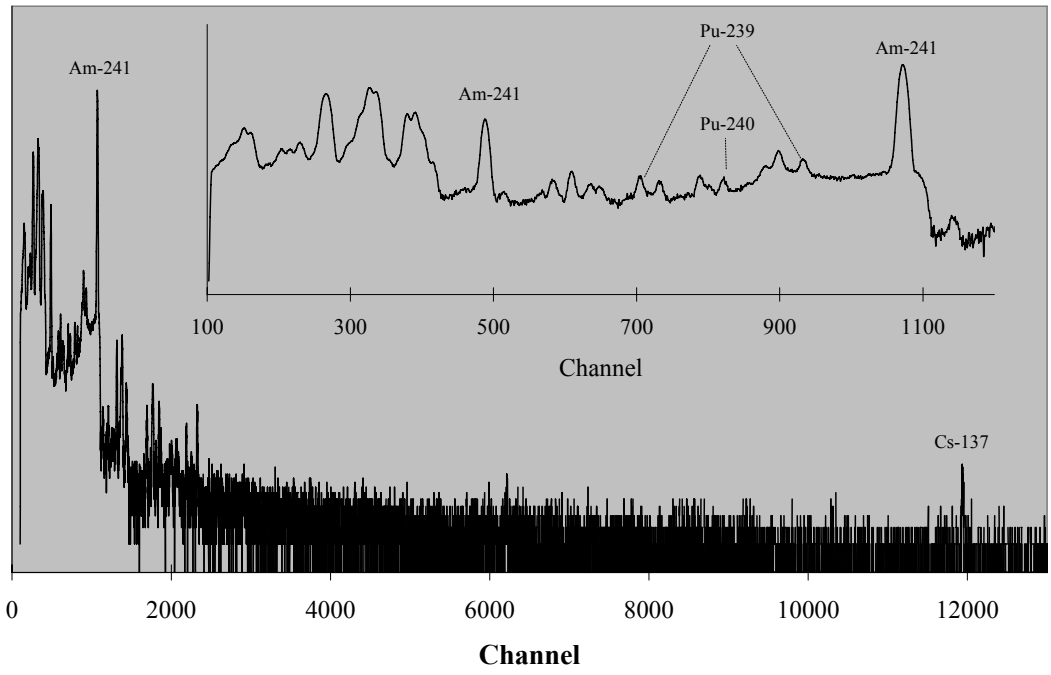
Am-241
Am-241
Pu-239
Pu-240
Am-241
100
300
500
700
900
1100
Channel
Cs-137
0
2000
4000
6000
8000
10000
12000
Channel

Figure 1.

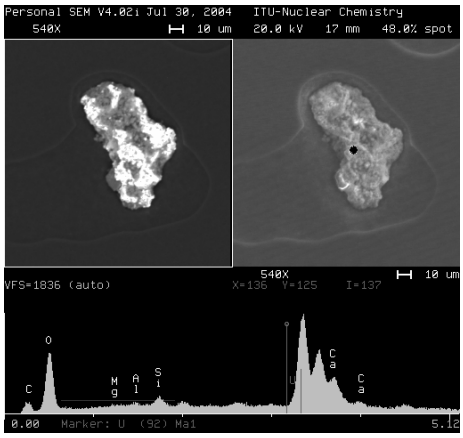
Personal SEM V4.02i Jul 30, 2004 ITU-Nuclear Chemistry
540X 10 um 20.0 kV 17 mm 48.0% spot
540X 10 um
VFS=1836 (auto) X=138 Y=125 I=137
O
C
Mg
Al
Si
U
Ca
Ca
0.00 Marker: U (92) Ma1 5.12

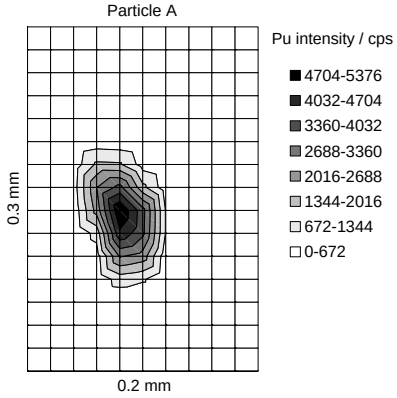
Particle A
Pu intensity / cps
4704-5376
4032-4704
3360-4032
2688-3360
2016-2688
1344-2016
672-1344
0-672
0.3 mm
0.2 mm

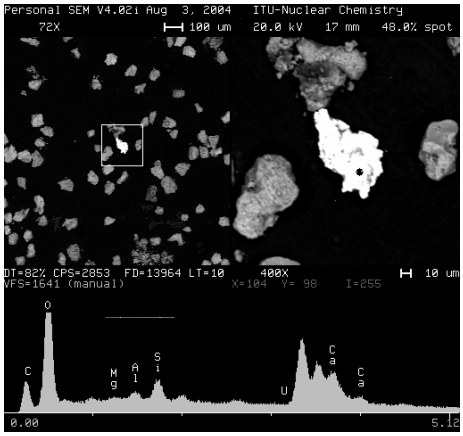
Personal SEM V4.02i Aug 3, 2004 ITU-Nuclear Chemistry
72X 100 um 20.0 kV 17 mm 48.0% spot
DT=82% CPS=2853 FD=13964 LT=10 400X 10 um
VFS=1641 (manual) X=104 Y= 98 I=255
O
C
Mg
Al
Si
U
Ca
Ca
0.00 5.12

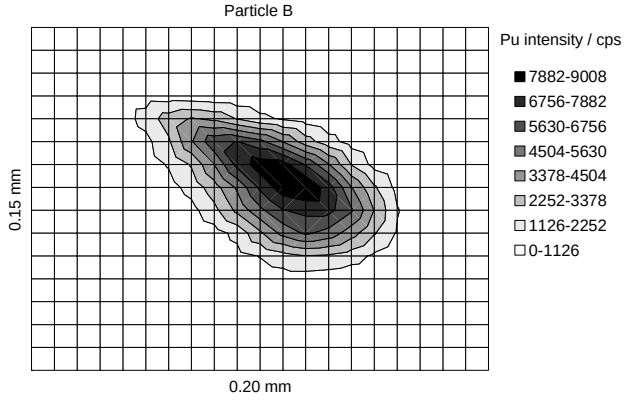
Particle B
Pu intensity / cps
7882-9008
6756-7882
5630-6756
4504-5630
3378-4504
2252-3378
1126-2252
0-1126
0.15 mm
0.20 mm

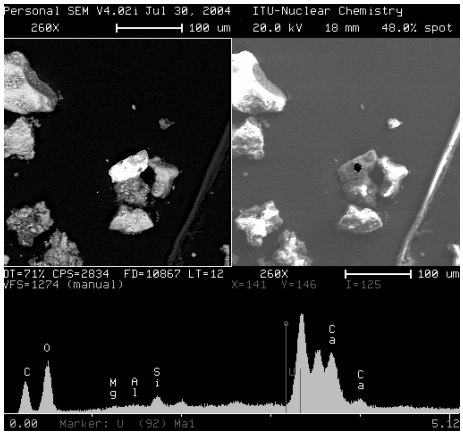
Personal SEM V4.02i Jul 30, 2004 ITU-Nuclear Chemistry
260X 100 um 20.0 kV 18 mm 48.0% spot
DT=71% CPS=2834 FD=10867 LT=12 260X 100 um
VFS=1274 (manual) X=141 Y=146 I=125
O
C
Mg
Al
Si
Ca
Ca
0.00 Marker: U (92) Ma1 5.12

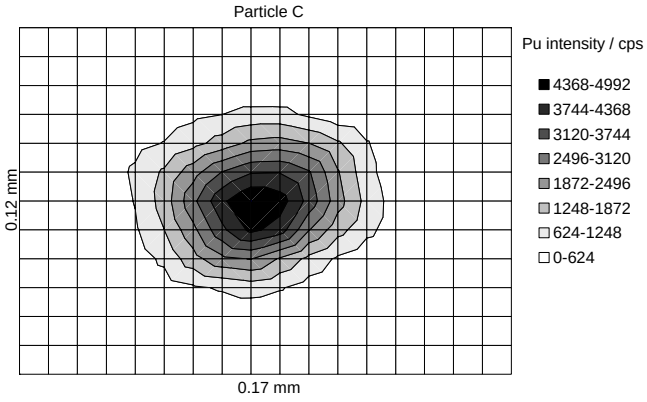
Particle C
Pu intensity / cps
4368-4992
3744-4368
3120-3744
2496-3120
1872-2496
1248-1872
624-1248
0-624
0.12 mm
0.17 mm

Figure 2a

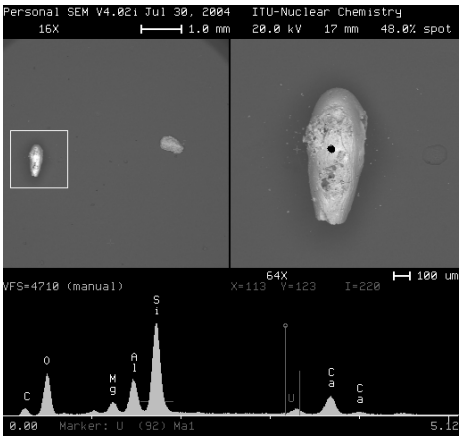
Personal SEM V4.02i Jul 30, 2004 ITU-Nuclear Chemistry
16X 1.0 mm 20.0 kV 17 mm 48.0% spot
64X 100 um
VFS=4710 (manual) X=113 Y=123 I=220
O
Si
Al
Mg
C
U
Ca
Ca
0.00 Marker: U (92) Mai 5.12

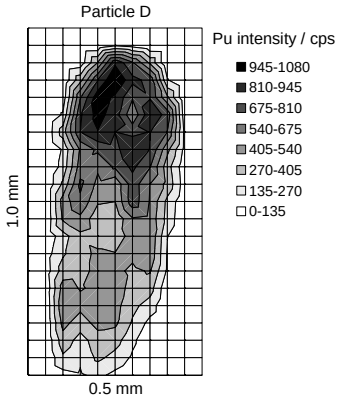
Particle D
Pu intensity / cps
945-1080
810-945
675-810
540-675
405-540
270-405
135-270
0-135
1.0 mm
0.5 mm

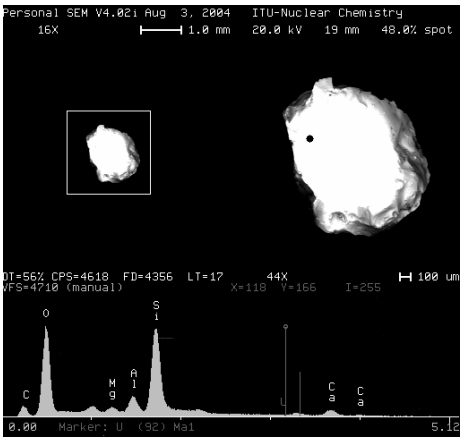
Personal SEM V4.02i Aug 3, 2004 ITU-Nuclear Chemistry
16X 1.0 mm 20.0 kV 19 mm 48.0% spot
DT=56% CPS=4618 FD=4356 LT=17 44X 100 um
VFS=4710 (manual) X=118 Y=166 I=255
O
Si
Al
Mg
C
U
Ca
Ca
0.00 Marker: U (92) Mai 5.12

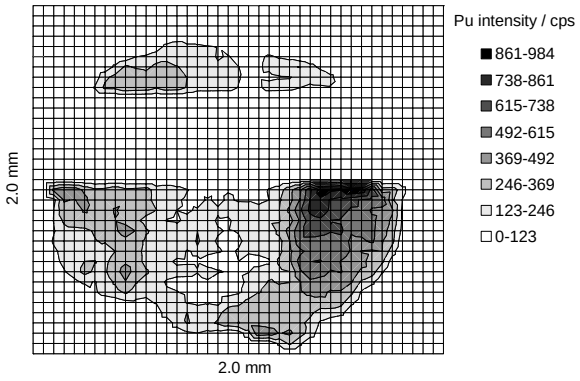
Particle E
Pu intensity / cps
861-984
738-861
615-738
492-615
369-492
246-369
123-246
0-123
2.0 mm
2.0 mm

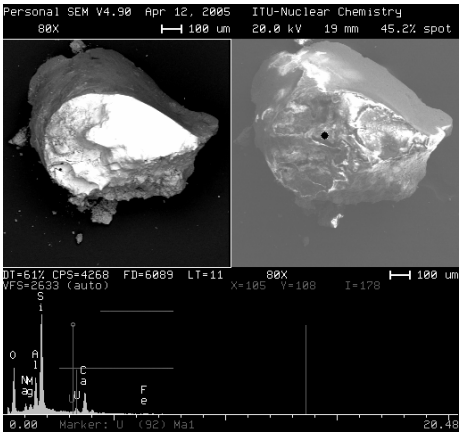
Personal SEM V4.90 Apr 12, 2005 ITU-Nuclear Chemistry
80X 100 um 20.0 kV 19 mm 45.2% spot
DT=61% CPS=4268 FD=6089 LT=11 80X 100 um
VFS=2633 (auto) X=105 Y=108 I=178
O
Si
Al
Mg
C
U
Ca
Fe
0.00 Marker: U (92) Mai 20.48

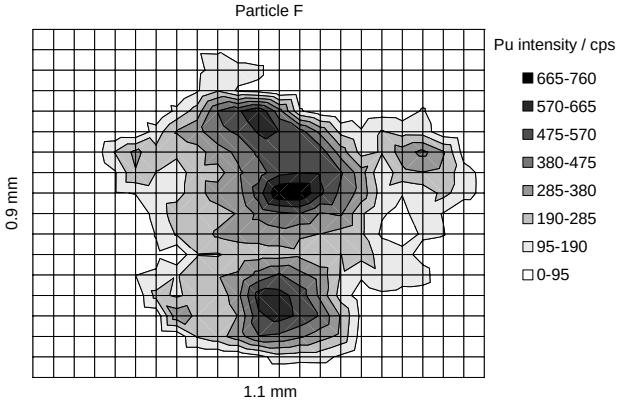
Particle F
Pu intensity / cps
665-760
570-665
475-570
380-475
285-380
190-285
95-190
0-95
0.9 mm
1.1 mm

Figure 2b

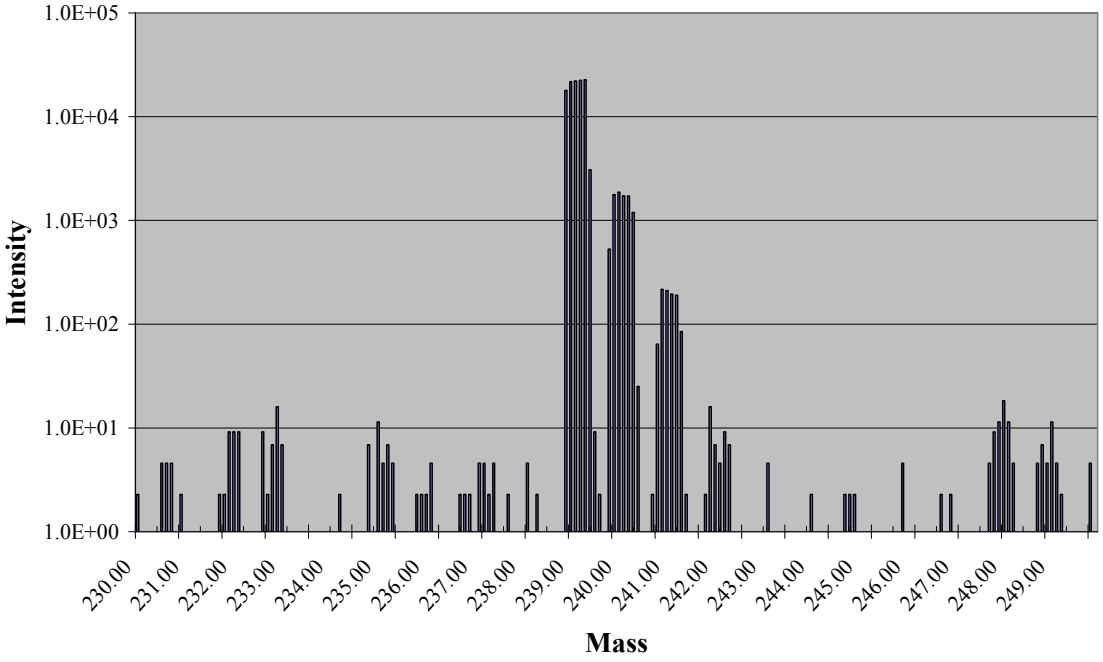
1.0E+05
1.0E+04
1.0E+03
1.0E+02
1.0E+01
1.0E+00
Intensity
230.00
231.00
232.00
233.00
234.00
235.00
236.00
237.00
238.00
239.00
240.00
241.00
242.00
243.00
244.00
245.00
246.00
247.00
248.00
249.00
Mass

Figure 3.